

Scalable multi-class sampling via filtered sliced optimal transport: Supplemental document

CORENTIN SALAÜN, Max-Planck-Institut für Informatik, Germany
 ILIYAN GEORGIEV, Autodesk, United Kingdom
 HANS-PETER SEIDEL, Max-Planck-Institut für Informatik, Germany
 GURPRIT SINGH, Max-Planck-Institut für Informatik, Germany

In this document we propose the derivation of the 1D 1-Wasserstein distance and additional results to the main document. You can find a second image of stippling in color for a lighthouse image. A monochrome stippling of elephants and an animation stippling example. We finally present two additional comparison for the rendering.

ACM Reference Format:

Corentin Salaün, Iliyan Georgiev, Hans-Peter Seidel, and Gurprit Singh. 2022. Scalable multi-class sampling via filtered sliced optimal transport: Supplemental document. *ACM Trans. Graph.* 41, 6, Article 261 (December 2022), 5 pages. <https://doi.org/10.1145/3550454.3555484>

S1 1D 1-WASSERSTEIN DISTANCE DERIVATIVE

Here we derive the derivative of the 1D Wasserstein distance for which has a closed-form exists [Rachev and Rüschendorf 1998]:

$$W_p^p(v, \mu) = \int_0^\infty |F_v^{-1}(x) - F_\mu^{-1}(x)|^p dx, \quad (1)$$

where F_v^{-1} and F_μ^{-1} are the measures' inverse CDFs. We are specifically interested in the case where $p = 1$ and one of the measures represents a 1D point set $X = \{x_i\}_{i=1}^n$. For this case we have

$$W_1^1(X, \mu) = \int_0^1 |(F_X^{-1}(x) - F_\mu^{-1}(x))| dx \quad (2)$$

$$= \sum_{i=1}^n \int_{\frac{i-1}{n}}^{\frac{i}{n}} |x_i - F_\mu^{-1}(x)| dx. \quad (3)$$

We want to differentiate this distance w.r.t. every point x_i . Only one of the integrals depends on each x_i :

$$\frac{d}{dx_i} W_1^1(X, \mu) = \begin{cases} \int_{\frac{i-1}{n}}^{\frac{i}{n}} 1 dx, & \text{if } (x_i - F_\mu^{-1}(x)) \geq 0 \\ \int_{\frac{i-1}{n}}^{\frac{i}{n}} -1 dx, & \text{otherwise} \end{cases} \quad (4)$$

Authors' addresses: Corentin Salaün, Max-Planck-Institut für Informatik, Saarbrücken, Germany, csalaun@mpi-inf.mpg.de; Iliyan Georgiev, Autodesk, United Kingdom, me@iliyan.com; Hans-Peter Seidel, Max-Planck-Institut für Informatik, Saarbrücken, Germany, hseidel@mpi-sb.mpg.de; Gurprit Singh, Max-Planck-Institut für Informatik, Saarbrücken, Germany, gsingh@mpi-inf.mpg.de.

Permission to make digital or hard copies of all or part of this work for personal or classroom use is granted without fee provided that copies are not made or distributed for profit or commercial advantage and that copies bear this notice and the full citation on the first page. Copyrights for components of this work owned by others than the author(s) must be honored. Abstracting with credit is permitted. To copy otherwise, or republish, to post on servers or to redistribute to lists, requires prior specific permission and/or a fee. Request permissions from permissions@acm.org.

© 2022 Copyright held by the owner/author(s). Publication rights licensed to ACM. 0730-0301/2022/12-ART261 \$15.00 <https://doi.org/10.1145/3550454.3555484>

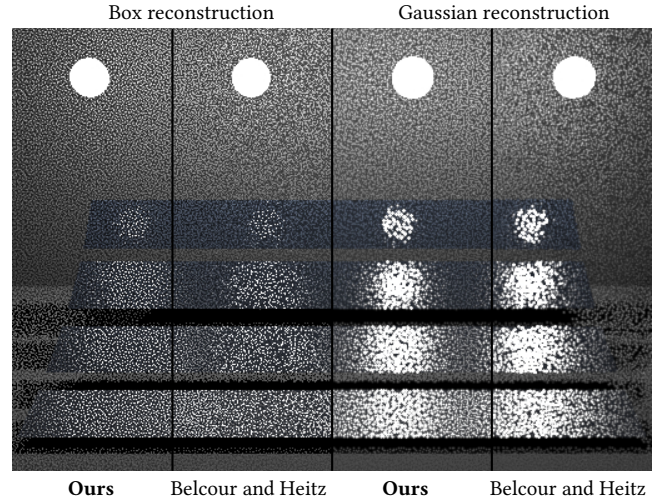


Fig. 1. Comparison between our perceptual error optimization and the blue-noise error distribution method of Belcour and Heitz [2021] using box and Gaussian pixel-reconstruction kernels. Our method achieves better quality in both cases.

The integral of the inverse target CDF is simply the average point inside the i^{th} region of the target density with mass $1/n$, multiplied by $1/n$. This derivative is only dependant of the sign of the difference $(x_i - F_\mu^{-1}(x))$ making it less attractive in a gradient descent algorithm.

S2 ADDITIONAL RESULTS RESULTS

Rendering comparisons. We show two additional results for rendering. Figure 1 shows the comparison of our method with Belcour and Heitz [2021] for rendering at 1 sample per pixel. On the right the comparison shows box reconstruction filter and on the right gaussian filter. We can see that our method performs better in both cases but this difference is more important for the gaussian filter. Contrary to Belcour and Heitz [2021] our method can be optimized for both the perceptual and the reconstruction filter. This difference leads to the improvement visible here.

Figure 4 shows two additional scenes for the integration error distribution comparing an uncorrelated rendering, Ahmed and Wonka [2020], Belcour and Heitz [2021] and our method. For this method we have displayed an image showing a power spectrum per tile in order to show the spectral distribution of the noise. We can see that our method results in the best noise distribution as it gets the fewest low frequencies.

Animated stippling. Figure 2 shows another example of stippling but across frames. Here we encode an entire sequence of 10 frames in a single point set. Each frame corresponds to one class with a trapezoidal function and a target distribution set to greyscale frame. There 75% of the points overlap between two consecutive frames leading to a large overlap in the class functions. That is, each frame is composed of 1,000 points and 250 of them are changed in the next frame. We have displayed 5 frames of the animation in Fig. 2 as well as the visualization of total point-set. This example shows the ability of the method to adapt the distribution of the points to jointly satisfy multiple objectives with overlap with different target distributions. A full animations is also available to better appreciate the multi-class nature of the problem.

Stippling. Figure 3 shows another example of color stippling for a lighthouse image with 40 000 points. The first line shows the complete result and the second one shows some classes.

Figure 5 is an example of monochrome stippling for an image of elephants. 100 000 points are used to generate this image.

REFERENCES

- Abdalla G. M. Ahmed and Peter Wonka. 2020. Screen-space blue-noise diffusion of Monte Carlo sampling error via hierarchical ordering of pixels. *ACM Trans. Graph.* 39, 6 (2020), 244:1–244:15. <https://doi.org/10.1145/3414685.3417881>
- Laurent Belcour and Eric Heitz. 2021. Lessons Learned and Improvements When Building Screen-Space Samplers with Blue-Noise Error Distribution. In *ACM SIGGRAPH 2021 Talks (Virtual Event, USA) (SIGGRAPH '21)*. Association for Computing Machinery, New York, NY, USA, Article 9, 2 pages. <https://doi.org/10.1145/3450623.3464645>
- Svetlozar Rachev and Ludger Rüschendorf. 1998. *Mass Transportation Problems: Volume I: Theory*. Springer.

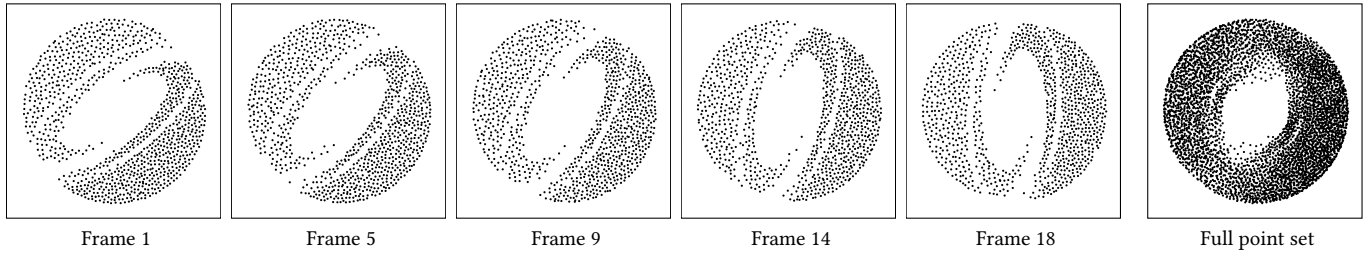


Fig. 2. Stippling of an 18-frame animation using 5,500 points. Each frame shows the 1,000 points inside an index window that moves by 250 points between consecutive frames; every point thus participates in four frames. Please see the supplemental animation to better appreciate the stippling motion.

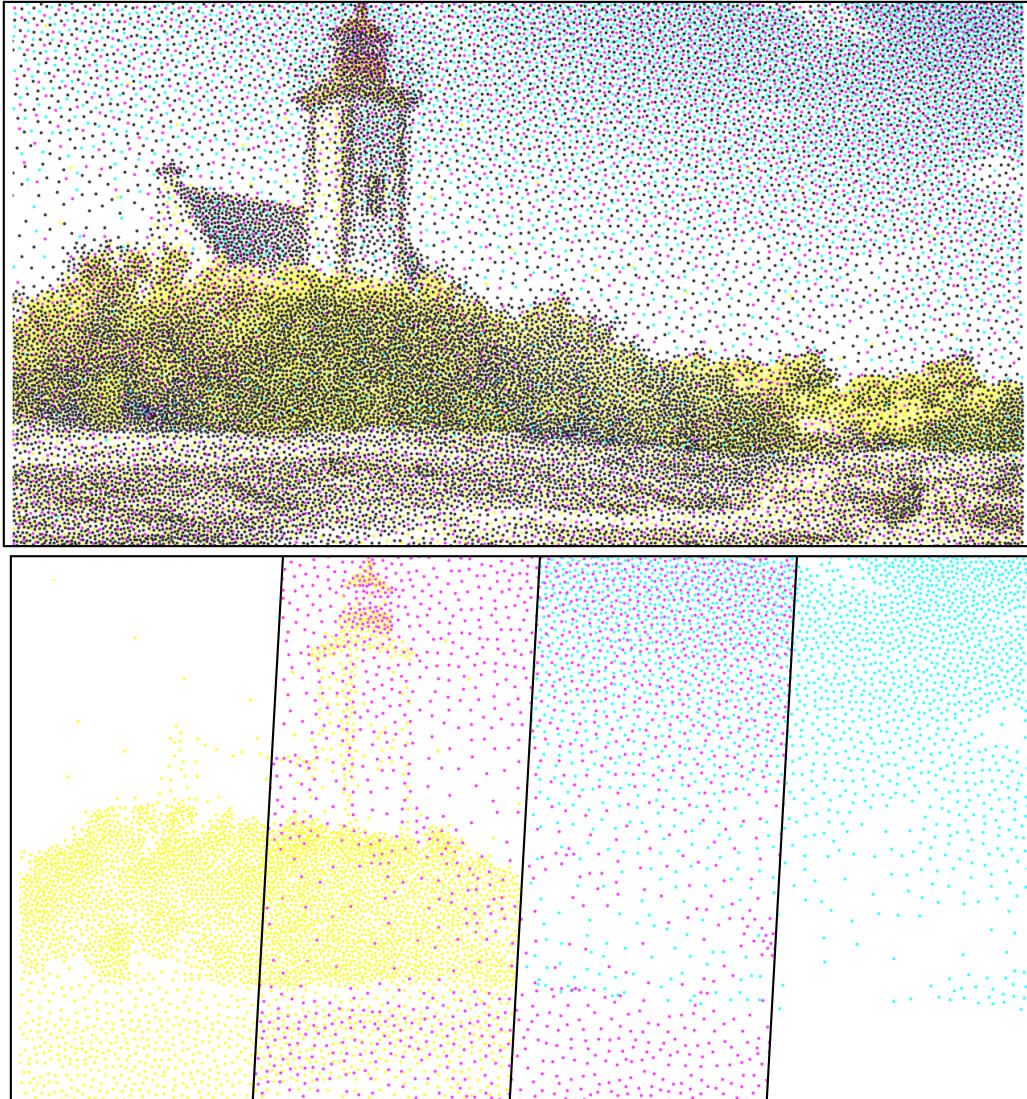


Fig. 3. Stippling image of a lighthouse using 4 colors (CMYK). The complete point-set is composed of 40 000 points and is visible on the top. On the bottom, we display some optimized classes, either individual colors or combinations. The complete problem is composed of 14 classes.

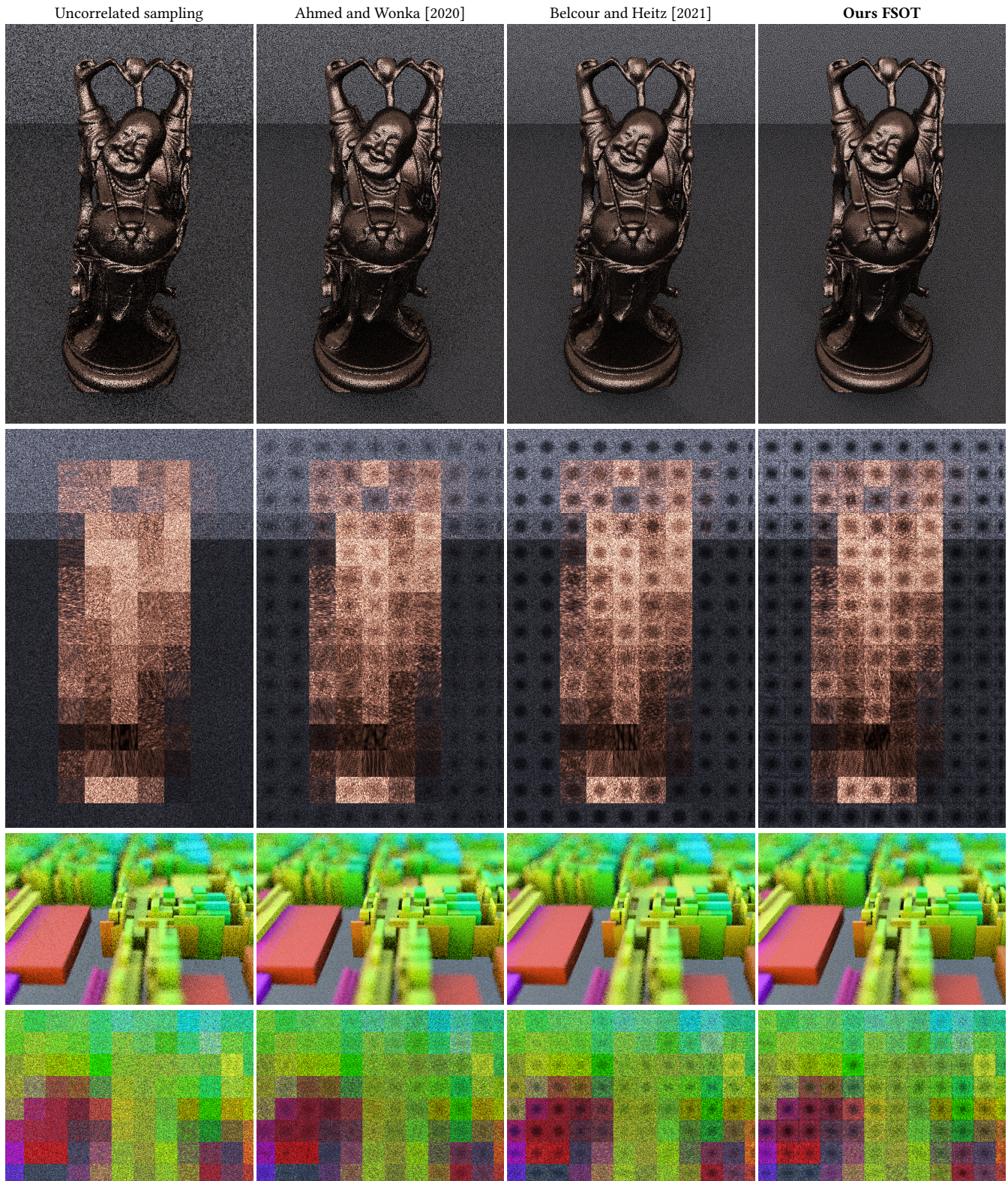


Fig. 4. Comparison of rendering our method with Ahmed and Wonka [2020] and Belcour and Heitz [2021]. The first line shows the rendering at 1 samples per pixel for the buddha scene and at 4 samples per pixel for the microcity scene. The second line shows the tiled power spectrum of the error with the reference.

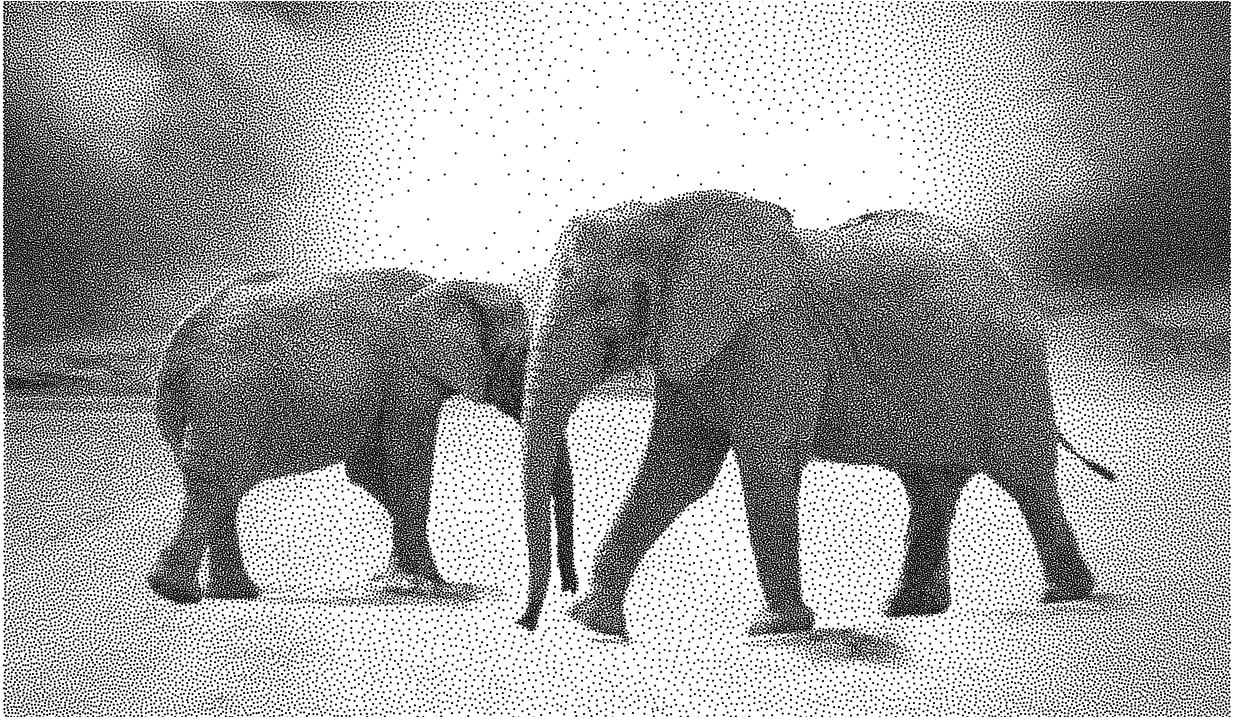


Fig. 5. Stippling image of elephants in grey scale. The point-set is composed of 100 000 samples optimized for a single class problem.